Theory and Practice of Science and Technology
2025, VOL. 6, NO. 6, 170-177
DOI: 10.47297/taposatWSP2633-456934.20250606

Design and Applications of a High-Precision Dual-Channel Microwave Latex Dry-Content Analyzer

Xin Chen

Hunan University of Science and Technology, Xiangtan, Hunan, 411201, China

ABSTRACT
The dry rubber content (DRC) is a critical parameter for assessing natural latex quality and determining its commercial value. Although conventional methods such as oven-drying offer high accuracy, they are labor-intensive, time-consuming, and impractical for rapid on-site applications. To overcome these limitations, this study introduces a high-precision, dual-channel DRC analyzer based on microwave dielectric attenuation principles.The system adopts a differential design to mitigate common-mode environmental interference, integrating high-sensitivity sampling chips and stable signal sources to enable fast, stable, and accurate DRC measurements. Through comparative analysis with industrial-grade standard equipment in both laboratory and field environments, the instrument demonstrated a controlled measurement error within 0.41%, exhibiting excellent repeatability and environmental adaptability. This innovation proves particularly suitable for field detection requirements in latex collection, trade transactions, and processing operations.

KEYWORDS
Dry Rubber Content (DRC); Microwave attenuation; Differential signal; High-precision measurement; Field detection

1 Introduction

The determination of dry rubber content (DRC) is pivotal in the production and processing of latex-based products, serving as a critical factor in procurement management and pricing strategies for enterprises within the latex industry[1]. Conventional DRC measurement methods, exemplified by the oven-drying technique[2], are characterized by labor-intensive procedures that demand specialized personnel controlled environments, rendering them incompatible with the efficiency requirements of modern industrial practices. Furthermore,The rubber industry's relatively closed ecosystem, combined with insufficient investment in R&D for detection technologies, has resulted in the widespread use of expensive yet technologically outdated instruments.This persistent innovation gap underscores an urgent need for portable, rapid, cost-efficient, and high-precision DRC analyzers to meet evolving industry demands.

Addressing this technological void, this study introduces a dual-channel DRC analyzer engineered on microwave attenuation principles. The instrument incorporates a differential circuit architecture to suppress environmental interference synergistically integrated with high-performance hardware components to achieve sub-0.5% measurement accuracy. Rigorous field evaluations conducted across multiple latex collection hubs in Hainan Province have validated its operational robustness, yielding repeatability errors below 0.41% under diverse ambient conditions. Beyond technical merits, this innovation democratizes DRC testing by enabling non-specialized personnel to perform on-site assessments in decentralized settings.This contributes to improved transparency and efficiency throughout the latex value chain—from raw material collection and trade negotiations to downstream processing—marking a significant advancement in quality control practices.

2 Theoretical background

2.1 Microphysical interaction mechanisms of microwave detection for latex dry content

The principle of microwave detection for latex dry content relies on the interaction between high-frequency electromagnetic waves and the material's microscopic components. When microwaves penetrate latex, two dominant energy dissipation mechanisms occur: ionic conduction loss and dipolar relaxation loss. Free ions (e. g., residual electrolytes in latex) migrate under the oscillating electric field, generating conductive currents that dissipate energy through ohmic heating. Simultaneously, polar molecules—particularly water—undergo rapid dipole reorientation at microwave frequencies, absorbing electromagnetic energy and converting it into thermal energy via dielectric relaxation. The attenuation of microwave signals correlates with the material's moisture content and ionic mobility, enabling quantitative dry content analysis by establishing a relationship between signal loss (attenuation coefficient) and the phase shift (dielectric dispersion) induced by these dual mechanisms.

2.2 Attenuation theory analysis of microwave detection for latex dry content based on maxwell's equations

According to Maxwell's equations[3], the propagation of electromagnetic waves in a medium can be mathematically described as follows: the electric field intensity E decays exponentially with propagation distance L and attenuation coefficient &, expressed as:

$$E=E_0*e^{\&L} \tag{1}$$

The total attenuation∀ is defined as the natural logarithm of the electric field intensity ratio, leading to the relationship between ∀ , L, and &:

$$\forall=\ln\left(\frac{E_0}{E}\right)=\ln\left(\frac{E_0}{E_0*e^{\&L}}\right)=\&*L \tag{2}$$

In this equation, the propagation distance L is a known parameter, while & remains unknown. For practical applications, latex is primarily a mixture of dry rubber and water, and & lacks a fixed reference value. Classical electromagnetic theory [4] indicates that & can be calculated using the real part of the permittivity i' (polarization characteristics) and the imaginary part i'' (loss characteristics):

$$\&=\frac{2\pi f i''}{c\sqrt{i'}} \tag{3}$$

where C is the speed of light.

Through mathematical modeling and experimental validation, three common methods for determining the effective permittivity of mixtures are identified: the Maxwell-Garnett model[5], Bruggeman effective medium theory[6], and the logarithmic mixing rule. Since the permittivity of water(ϵ_{water}) is significantly higher than that of dry latex (ϵ_{latex}) the attenuation coefficient & is inversely proportional to latex concentration. Consequently, when L is fixed, an increase in latex concentration reduces the total attenuation ∀, establishing a quantifiable basis for dry content detection.

2.3 Theoretical validation

The experimental setup is illustrated in Figure 1. A microwave signal generated by the source passes through an isolator and propagates via a waveguide to interact with the test material. The total attenuation is measured by detecting the voltage change after the signal passes through a second isolator, where attenuation is quantified as the voltage difference between the transmitted and reference signals.

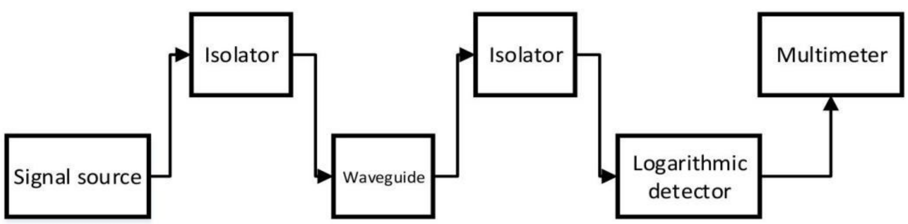

Figure 1 Theoretical validation flowchar

Using a 9.35 GHz microwave signal, two experimental setups were compared:Experiment 1 (without water column): No water column was placed in the waveguide.Experiment 2 (with water column): A water column with an outer diameter of 6 mm was inserted into the waveguide.The input microwave power was varied to simulate changes in moisture content. Repeated tests were performed, and the integrated data were plotted as the scatter diagram in Figure 2.

Key findings include:Voltage contrast: The output voltage in Experiment 2 (with water column) was significantly higher

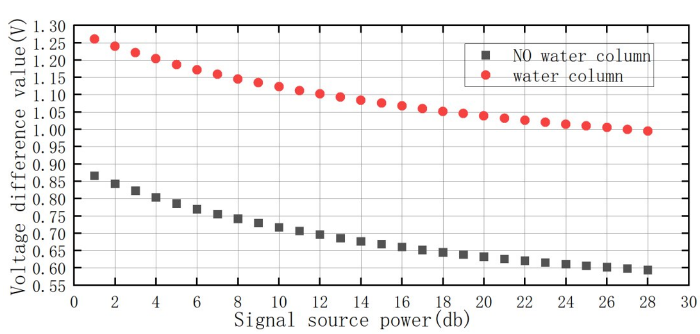

Figure 2 Scatter plot of theoretical test data validation

than in Experiment 1 (without water column). This directly confirms that water molecules absorb microwave energy, aligning with the theoretical mechanism of dielectric loss. Power-dependent voltage decline: In both experiments, the output voltage decreased as the input microwave power increased. This trend demonstrates that the system's response (voltage) correlates with input power variations, which simulate moisture content changes. Experimental consistency: The inverse relationship between input power and output voltage under both conditions validates the reliability of the attenuation model derived from Maxwell's equations.

This comparative analysis robustly verifies the theoretical framework for microwave-based detection of latex dry content, emphasizing the critical role of water's dielectric properties in signal attenuation.

3 Circuit design workflow

The overall circuit design workflow is illustrated in Figure 3. The microcontroller unit (MCU) controls the microwave signal source to transmit signals. The attenuated microwave signals, after passing through the circuit, are fed back to the MCU via a sampling chip in the form of voltage differentials. The MCU processes and analyzes the received data to quantify attenuation characteristics. A display module directly presents the final results, ensuring intuitive readability for operators. Additionally, the system supports remote data transmission and monitoring through MODBUS_RTU protocol communication with a host computer, enabling real-time industrial oversight and centralized data management.

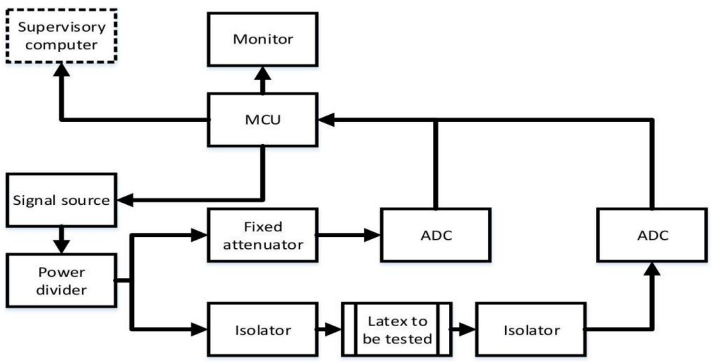

Figure 3 Overall flowchart

3.1 Design of main hardware circuit

Currently, most domestic markets employ single-channel microwave detection methods for latex dry content measurement. Although this approach can provide concentration data, the detection results are significantly affected by environmental factors.

To address this issue, the proposed design adopts a low-cost differential circuit[7-8] to effectively compensate for potential circuit errors, thereby enhancing the accuracy and stability of the equipment. The system utilizes a power splitter to divide the microwave signal into two paths: one serves as the test group passing through the latex sample, while the other functions as the control group through a fixed attenuator (simulating a known attenuation environment). The dry content is then calculated precisely based on the voltage difference between these two paths. According to the principle of differential signals, common-mode interference caused by environmental variations (e.g., temperature and humidity fluctuations) will simultaneously affect both the test and control groups, generating common-mode signals. The inherent characteristics of the differential circuit enable effective suppression of such common-mode signals. Consequently, the voltage difference error is substantially reduced, leading to significant improvements in both measurement accuracy and stability for latex dry content detection.

3.2 Core component selection and performance optimization

3.2.1 Main control chip

The main control chip primarily handles data processing and module coordination. This study employs the STM32F103RCT6 microcontroller[9-10], widely available in the commercial market for its accessibility. With a maximum data transfer rate of 18 MHz and a single transmission duration of approximately 1.33 μs, this chip demonstrates high efficiency in rapid data processing and transmission tasks. Furthermore, its cost-effectiveness significantly reduces hardware expenditures during project development. The STM32F103RCT6 also exhibits exceptional flexibility, enabling seamless functional expansion and customized instrument development tailored to diverse application scenarios and requirements.

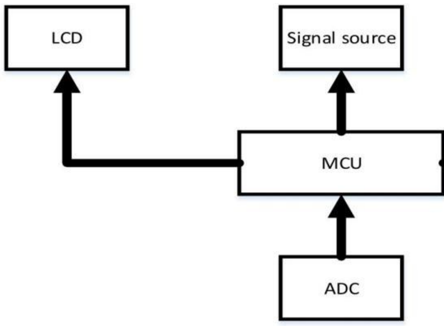

Figure 4 Main control module

3.2.2 Signal source selection and logarithmic detector

When applying the microwave attenuation principle to moisture content detection, the primary challenge lies in determining an appropriate microwave signal frequency. According to References [11][12][13][14], the performance parameters of microwaves at different frequencies are summarized in Table 1. The data reveal that the 3.2 GHz frequency exhibits balanced characteristics across key metrics, including dielectric constant, dielectric loss, temperature stability, and penetration depth.

Table 1 :Performance comparison of microwave frequencie

Frequency Parameter	0.915 GHz	2.4 GHz	3.2 GHz	8.5–14.5 GHz
Dielectric loss factor (ε")	~10	~13	~14	15–20
Dielectric constant (ε')	80	77	72	50–60
Penetration capability	High	Medium	Medium	Low
Temperature stability	Low	Medium	High	Low

Specifically, compared to lower frequencies (0.915 GHz), 3.2 GHz demonstrates moderately high dielectric constant (~ 72) and dielectric loss factor (~13), which enhances the sensitivity of the sensor response, albeit with a slight reduction in penetration capability. Furthermore, its superior temperature stability ensures consistent detection accuracy under environmental temperature fluctuations. In contrast to higher frequency bands (8.5 – 19.5 GHz), the 3.2 GHz frequency exhibits relatively lower dielectric loss, thereby mitigating excessive signal attenuation and temperature rise caused by energy absorption while retaining adequate sensitivity.

Consequently, by comprehensively evaluating microwave propagation properties in materials and sensor performance requirements, 3.2 GHz emerges as an optimal frequency for dielectric detection applications, offering an effective compromise between stability and sensitivity.

Given the frequency sensitivity of dielectric constant measurements, minor frequency deviations may introduce errors in attenuation coefficient calculations. Therefore, the signal source must demonstrate exceptional stability. This design employs the LMX2592[14][15] phase-locked loop (PLL) as the signal source, which offers wide frequency coverage and seamless frequency switching, eliminating subsequent circuit adjustments. Additionally, the LMX2592 features superior signal shielding capabilities.

A cost analysis was conducted across major markets (e.g., Texas Instruments, JD.com), with results shown in Table 2. Although the unit price of LMX2592 is ~45% higher than the conventional ADF4351 chip, its performance significantly outperforms the latter. The LMX2592's high integration reduces peripheral circuit requirements, thereby minimizing hidden costs associated with calibration, shielding, and re-testing. The total cost difference ranges only 10–15%.

Table 2 Cost-performance comparison between LMX2592 and ADF4351

Chip	Unit Price (USD)	Peripheral Circuits (USD)	Total Cost (USD)	Rationale
LMX2592	80-120	50-80	130-200	High integration reduces external circuits
ADF4351	10-15	80-120	90-135	Lower accuracy necessitates additional filtering circuits

A logarithmic detector (AD8319[16-17]) was selected for output signal detection. The LMX2592-AD8319 combination provides an end-to-end optimized solution for latex dry-content measurement, meeting this design's stringent requirements for real-time performance, stability, and miniaturization.

As shown in Table 3, while the initial cost difference between the AD8319-based solution and traditional multi-stage detection circuits is <10%, the integrated design reduces maintenance costs (60% lower failure rate) and extends service intervals from 2 weeks to 6 months. Error analysis confirms a 4× precision improvement over conventional ADF4351 solutions.

Table 3 Cost comparison: AD8319 vs. multi-stage detection circuits

Component	AD8319 Solution (USD)	Multi-stage Circuit[18] (USD)
Detector	12-18	20-30
Peripheral circuits	50–80 (filtering+calibration)	100–150 (filtering+calibration)

3.2.3 Sampling chip

The TM7707 chip was selected for sampling in this design. This chip integrates an on-chip PTAT temperature sensor that enables real-time correction of the 2.5V reference voltage (±5ppm/°C). Combined with background calibration, it effectively mitigates thermal hysteresis effects, ensuring measurement stability across varying temperature conditions.

The built-in low-drift oscillator (drift rate: ±0.005%) operates synergistically with a $sinc^3$ digital filter to suppress clock noise. The cutoff frequency of the digital filter is programmable within 10Hz–2.4kHz, allowing adaptive noise suppression in the frequency domain through register configuration. This feature simplifies system design by eliminating the need for additional external circuits.

Given that latex collection often occurs in outdoor high-temperature environments (e.g., Hainan), where temperature fluctuations significantly impact measurement accuracy, the TM7707 chip provides a robust solution for precision measurements in such scenarios through the aforementioned characteristics

3.2.4 Power supply module

This design employs the lithium battery BQ24610[19][20] as the power management module. Characterized by high integration, this module reduces external hardware components while enhancing the reliability and stability of the system's power supply. It exhibits excellent environmental adaptability, dynamically switching operational modes based on ambient conditions to ensure both battery safety and efficient utilization. Furthermore, the module optimizes coordination with the system controller, thereby improving overall developmental performance. In terms of endurance, it demonstrates prolonged energy storage capacity.

Regarding cost, the BQ24610-based solution reduces total expenses by approximately 28% compared to conventional alternatives. This approach aligns with the study's core objectives of low cost, portability, and high stability, providing an economically viable power solution for the design of latex dry-content detection instruments.

4 Software design

In the software design phase, the calibration and compensation testing procedure is indispensable for ensuring the accuracy of system concentration measurements[21][22]. As illustrated in Figure 5, this workflow systematically outlines the process from data acquisition to final formula correction.

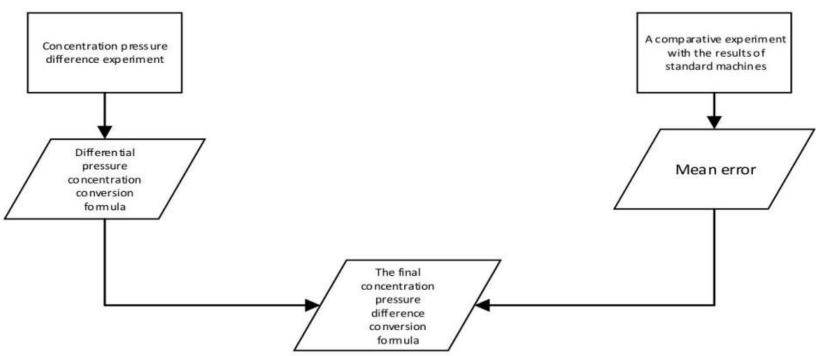

Figure 5 Calibration and Compensation Testing Procedure

4.1 Derivation of pressure difference-concentration conversion formula

The dilution method[23-24] was employed to establish the pressure difference-concentration conversion formula, with ambient temperature held constant while latex concentration was varied. During operational configuration, precise records were maintained for the beaker weight, initial latex weight, and added water weight to minimize measurement errors affecting subsequent results.

To visualize the correlation between voltage and concentration, the data from Table 4 were plotted as a scatter diagram (Figure 6), where the X-axis represents latex concentration (unit: M) and the Y-axis denotes pressure difference (mV).

Table 4 Pressure Difference vs. Concentration Dataset

Calibration usage						
Adhesive temperature	Ambient temperature	Theoretical concentrationM	Weight before adding water	Weight after adding water	Initial value	Voltage difference ΔV
26.2	25.8	38.24	203.2	213.2	25.9	114.8
		36.44637899	200.9	210		124.5
		34.8670359	201.2	212		133.1
		33.09079067	200	210.6		143.1
		31.4252523	200	210.3		153.1
		29.88611726	203.4	213.1		162.6
		28.52574496	200	210		172
		27.16737615	199.7	209.2		182.2
		25.93367599	201.2	211		191.4
		24.72917351	191.3	201.5		201
		23.47737415	195.5	205.3		210.8

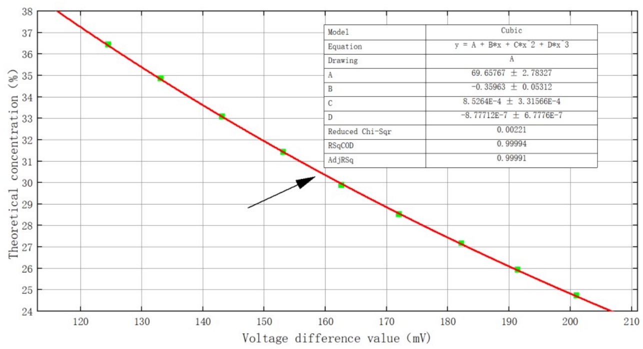

Figure 6 Scatter Plot of Pressure Difference vs. Concentration

The fitted curve demonstrated a reliability coefficient >0.99, indicating excellent fitting performance. The resultant conversion formula, with pressure difference ΔV as the independent variable (X-axis) and derived concentration M as the dependent variable (Y-axis), is expressed as:

$$M=(-8.78\times10^{-7}\pm6.78\times10^{-7})\Delta V^3+(8.53\times10^{-4}4\pm3.32\times10^{-4})\Delta V^2+(-0.3596\pm0.0531)\Delta V + (69.66\pm2.78) \quad (4)$$

4.2 Concentration error calibration

To ensure the accuracy of the designed system in measuring latex concentration, comparative testing was conducted under identical environmental conditions using an industrial-grade reference instrument. Error compensation was performed based on repeated large-scale data comparisons. The test results are presented in Table 5.

Table 5 Comparative Test Data vs. Standard Instrument

Env. Temp. (°C)	Initial Value	Voltage Diff	Calculated Conc. (M)	Reference Conc.	Displayed Conc. (M)	Ref. - Calc. Conc	Ref. - Displayed Conc.
26.21244562	19.8	168.9	25.86299565	26.33	25.87	0.46700435	0.46
26.25741948	19.8	160.1	27.15659356	27.42	27.16	0.263406441	0.26
26.30096786	19.8	152.7	28.26007743	28.61	28.26	0.349922572	0.35
26.30232941	19.8	151.7	28.41018635	28.71	28.41	0.299813647	0.3
26.31478972	19.8	167.2	26.11118318	26.28	26.11	0.168816823	0.17
26.28738225	19.8	179.9	24.27899058	24.63	24.28	0.35100942	0.35
26.31734841	19.8	172.7	25.31138787	25.79	25.31	0.478612127	0.48
26.30031149	19.8	176.6	24.75002492	25.04	24.75	0.289975081	0.29
26.39464146	19.8	166.2	26.25757132	26.59	26.25	0.332428683	0.34
26.37293344	19.8	173.5	25.19583468	25.61	25.19	0.414165325	0.42
26.42129578	19.8	166.8	26.16970366	27	26.16	0.830296338	0.84
26.36253363	19.8	187.6	23.19500269	23.7	23.19	0.504997309	0.51
26.31506299	19.8	164.2	26.55120504	27.02	26.55	0.468794961	0.47
26.31985318	19.8	156.3	27.72158825	28.12	27.72	0.398411746	0.4
26.35192227	19.8	161.4	26.96415378	27.26	26.96	0.295846219	0.3
26.41132396	19.8	158.4	27.40890592	27.5	27.4	0.091094083	0.1

Statistical analysis revealed: Mean deviation between calculated and reference concentrations: 0.38. Mean deviation between displayed and reference concentrations: 0.38.

Building upon the pre-established pressure-concentration conversion formula, the mean error values were incorporated to enhance accuracy. The compensated conversion formula is expressed as:

$$M=(-8.78\times10^{-7}\pm6.78\times10^{-7})\Delta V^3+(8.53\times10^{-4}4\pm3.32\times10^{-4})\Delta V^2+(-0.3596\pm0.0531)\Delta V+(69.66\pm3.16) \quad (5)$$

5 Application and verification

Field testing was conducted in outdoor environments with ambient temperatures ranging from 17° C to 35° C. The schematic of the test prototype is illustrated in Figure 7.

Figure 7 Test prototype

Three machines were deployed for the evaluation, yielding 293 standardized test datasets (one calibration dataset per machine excluded from statistical analysis). Systematic statistical processing of these data produced the error distribution results summarized in Table 6.

Table 6 Error statistics of test results

Error Range	Sample Count	Percentage	Mean Error	Weighted Error
⩽0.1	45	15.36%	0.05	0.007679181
0.1<X⩽0.3	103	35.15%	0.2	0.070307167
0.3<X⩽0.5	56	19.11%	0.4	0.076450512
0.5<X⩽1	75	25.60%	0.78	0.191979522
1<X⩽1.5	12	4.10%	1.25	0.051194539
1.5<X⩽2	2	0.68%	1.75	0.011945392
Total	293	100.00%		
			Cumulative Weighted Error	0.409556314

5.1 Key conclusions

field test results demonstrate that the latex dry-content analyzer achieves a high measurement throughput of over 200 samples per hour with a sub-second detection time per sample (<1 s), while maintaining exceptional repeatability (0.05% – 0.1% error range) and robust precision evidenced by a cumulative weighted error of 0.41%. The device operates effectively across a concentration range of 10% – 50% without stringent sample volume requirements, ensuring operational flexibility in diverse environments, and exhibits reliable performance under ambient temperatures between 17° C and 35° C for both indoor and outdoor applications. Powered by AC 220V (50Hz ±10%) with backup battery capability for short-term mobility, its compact design (400×363×97 mm) and lightweight construction (5 kg) enhance portability, making it suitable for field deployments requiring rapid, accurate latex analysis under standard conditions.

5.2 Additional notes

Limitations: Errors exceed 1% when temperature or concentration ranges deviate from specified thresholds. Dual-Channel Advantage: Compared to single-channel models, the dual-channel design reduces mean error by 0.1049%. Further precision enhancements (e. g., advanced circuit monitoring) were deemed unnecessary for mainstream applications.

6 Conclusion

The latex dry-content analyzer employs an all-digital circuit architecture, featuring rapid startup, temperature drift resistance, and an MCU-driven LCD interface. Customizable software algorithms allow adaptability to diverse requirements. Post-calibration standardization may enable batch utilization, improving production efficiency.

While the 0.41% mean error meets general demands, extreme-environment performance and narrower detection ranges (10%–50%) warrant future optimization. Prospective work should focus on:Precision enhancement through design refinements.Extended operational limits (e.g., broader temperature/concentration ranges).

About the Author

Xin Chen, 18169322824@163.com.

References

[1] HERATH K D. Discovering the Properties of Natural Rubber Latex[J]. 2021.

[2] Tillekeratne L M K, Karunanayake L, Kumara P H S, et al. A rapid and accurate method for determining the dry rubber content and total solid content of NR latex[J]. Polymer Testing, 1988, 8(5): 353-358.

[3] Huray P G. Maxwell's equations[M]. John Wiley & Sons, 2009.

[4] Pozar D M. Microwave engineering[J]. Fourth Editions, University of Massachusetts at Amherst, John Wiley & Sons, Inc, 2012: 26-30.

[5] Markel V A. Introduction to the Maxwell Garnett approximation: tutorial[J]. Journal of the Optical Society of America A, 2016, 33(7): 1244-1256.

[6] Goncharenko A V. Generalizations of the Bruggeman equation and a concept of shape-distributed particle composites[J]. Physical review E, 2003, 68(4): 041108.

[7] Dash S K, De B P, Appasani B, et al. Design of a optimized CMOS Differential Amplifier using Craziness-based PSO[J]. Journal of VLSI Circuits and Systems, 2025, 7(1): 26-31.

[8] Alijani M, Javanmardi M, Abrishamifar A. A wide tuning range CMOS differential ring VCO using an active inductor for wireless applications[J]. International Journal of Circuit Theory and Applications, 2025, 53(3): 1171-1183.

[9] Zheng J, Mao H, Wang X, et al. Design of an IoT-based domestic control system[C]//International Conference on Mechatronic Engineering and Artificial Intelligence (MEAI 2024). SPIE, 2025, 13555: 329-333.

[10] Zheng J, Mao H, Wang X, et al. Design of an IoT-based domestic control system[C]//International Conference on Mechatronic Engineering and Artificial Intelligence (MEAI 2024). SPIE, 2025, 13555: 329-333.

[11] Vijay R, Jain R, Sharma K S. Dielectric properties of water at microwave frequencies[J]. International Journal of Engineering Research & Technology (IJERT), 2014, 3(3): 1452–1456.

[12] Xiao H, Huang J, Wang M, et al. Unraveling molecular loss processes for dielectric polymers in the Terahertz frequency range: Impact of polarity and chain rigidity[J]. Polymer, 2024, 297: 126855.

[13] Komarov V. Dielectric permittivity and loss factor of tap water at 915 MHz[J]. Microwave and Optical Technology Letters, 2004.

[14] Meredith R J. Engineers' Handbook of Industrial Microwave Heating[M]. London: Institution of Engineering and Technology, 1998.

[15] Ortega E, Martínez A, Oliva A, et al. A Digital Beamforming Receiver Architecture Implemented on a FPGA for Space Applications[J]. arXiv preprint arXiv:2405.18992, 2024.

[16] Kennedy M P, Lu X, Wang X. Insights into architectural spurs in high performance fractional-N frequency synthesizers[J]. IEEE Open Journal of the Solid-State Circuits Society, 2024.

[17] DELL'ACQUA A. Sviluppo e validazione di un sistema per la regolazione automatica della potenza di un segnale a microonde in un apparato per il controllo di qubit superconduttori[J]. 2025.

[18] Khadem M S, Rezaei Borjlu S, Makkiabadi B. An Efficient Frequency Compensation Approach for Multi - Stage CMOS Amplifiers[J]. International Journal of Numerical Modelling: Electronic Networks, Devices and Fields, 2025, 38(3): e70024.

[19] Fang G, Xu Q, Wang W, et al. Development of Novel Transient Fault Recording System Used in Distribution Network[C]//2022 3rd International Conference on Advanced Electrical and Energy Systems (AEES). IEEE, 2022: 425-430.

[20] Lee S W. Design Example to Charge Three Super Capacitors in Series with Health Monitoring Using bq24610 and bq33100[J]. 2020.

[21] Gu T, Yuan S, Gu L, et al. Research on dynamic calibration and compensation method of strain-gauge type force sensor[J]. Sensor Review, 2024, 44(1): 68-80.

[22] Gruber G, Schweighofer B, Berger M, et al. Eddy current position measurement in harsh environments: A temperature compensation and calibration approach[J]. Sensors, 2024, 24(5): 1483.

[23] Kitanidis P K. The concept of the dilution index[J]. Water resources research, 1994, 30(7): 2011-2026.

[24] Jones W B, Donati G L, Calloway Jr C P, et al. Standard dilution analysis[J]. Analytical chemistry, 2015, 87(4): 2321-2327.